CrossMark

ORIGINAL

# Isolation and characterization of bagasse cellulose nanofibrils by optimized sulfur-free chemical delignification

**Pejman Heidarian**[1] · **Tayebeh Behzad**[1] ·
**Keikhosro Karimi**[1]

**Abstract** Cellulose nanofibril (CNF) was isolated from bagasse using a modified sulfur-free and bio-refinery-based approach. For this purpose, a chemo-mechanical procedure was designed that consisted of depithing, de-waxing, autohydrolyzing, soda-anthraquinone pulping, elemental chlorine-free bleaching, refining, and ultrafine grinding. In order to obtain a high degree of final fibrillation, the most important parameters in the delignification process were optimized by response surface methodology. Samples were then characterized by optical microscopy, scanning electron microscopy, X-ray diffraction (XRD), National Renewable Energy Laboratory procedure, ASTM (D1103-60 and D1104-56), Kappa number, Fourier transform infrared spectroscopy (FTIR), dynamic light scattering (DLS), and transition transmission electron microscopy (TEM). The microscopic images as well as the results from chemical composition characterization and FTIR analysis indicated that the employed chemical treatments were effective in removing non-cellulosic materials from the fibers. In addition, XRD analysis showed that cellulose crystallinity increased during the treatments. Based on the DLS results, the hydrodynamic diameter of CNF ranged within 860 nm. TEM image analyses showed that a considerable percentage of the isolated CNF had an average diameter of about 11 nm, and the yield of fibrillation was found to be about 99 %. Based on the results obtained, it may be claimed that the chemo-mechanical process developed in this study for the facile preparation of CNF is a promising technique for biocomposite preparation.

✉ Pejman Heidarian
p.heidarian@ce.iut.ac.ir; tbehzad@cc.iut.ac.ir

[1] Department of Chemical Engineering, Isfahan University of Technology, Isfahan 84156-83111, Iran

🖄 Springer

# Introduction

In the contemporary, advanced green nanotechnology, increasing attention is being directed toward the development of new methods for isolating nanocellulosic materials from agro-industrial waste residues such as bagasse (Hassan et al. 2012; Li et al. 2012; Mandal and Chakrabarty 2011; Teixeira et al. 2011). Indeed, bagasse is a fibrous residue obtained from crushing sugarcane stalks during the sugar extraction process (Mandal and Chakrabarty 2011; Teixeira et al. 2011), and the same as hardwoods, bagasse has short fiber lengths with pentoses and syringyl–guaiacyl units in the main structures of hemicellulose and lignin, respectively (Hassan et al. 2012). Generally, the bagasse fibers contain two main parts, involving 70–75 % outer rinds and 30–35 % undesirable inner piths. The piths consist of soft materials such as small fibers and sucrose, while rinds contain larger and finer fibers (Casey 1952). It was reported that the range of cellulose, hemicelluloses, and lignin content in the bagasse is about 40–50, 20–35, and 18–24, respectively (Mandal and Chakrabarty 2011). Overall, the bagasse is an abundant, inexpensive, and readily available lignocellulosic source for isolating such nanocellulosic biomaterials as cellulose nanofibrils (CNF).

Generally, microfibrils consist of nanofibrils that form the building blocks of plant cell walls, called elementary fibrils. They are packed in primary and secondary cell walls and are surrounded by hemicellulose, lignin, and extractives (Dufresne 2013). Cellulose microfibrils within a range of 2–20 nm in diameter are formed during the biosynthesis process and provide a natural reinforcement for the plant's stability (Thomas and Pothan 2009). They consist of a linear chain with about 30–100 cellulose molecules formed of repeating $\beta$-1-4-linked D-glucopyranose units (Kalia et al. 2011). The major portion of the oriented cellulose microfibrils exists in the secondary cell walls to form what are called the "crystalline regions" (Sun 2010). Therefore, the disintegration of the cellulose microfibrils requires methods of high shear mechanical fibrillation with a high energy demand such as the high-pressure homogenizer and/or ultrafine grinder (Dufresne 2013; Hassan et al. 2012; Li et al. 2012) which are not economically feasible for industrial scale applications (Dufresne 2013; Zhang et al. 2013).

A number of studies have been conducted on the isolation of nanocellulose from bagasse with various pre- and post-treatments (Mandal and Chakrabarty 2011; Teixeira et al. 2011) and even their optimization (Hassan et al. 2012; Li et al. 2012). Mandal and Chakrabarty (2011) used acid hydrolysis to isolate nanocellulose from bagasse fibers. For this purpose, they used sodium chlorite and sodium hydroxide solutions as bleaching and pulping agents followed by strong acid hydrolysis by refluxing with 60 % (w/v) sulfuric acid. Their results indicated that the obtained nanocellulose after acid hydrolysis had nanodimensions in the range of 70–90 nm.

Teixeira et al. (2011) used bagasse to obtain whiskers via alkaline peroxide pretreatment followed by acid hydrolysis procedure. They also probed the influence of extraction time on the properties of the nanofibers. Their results indicated that cellulose whiskers had needle-like morphology with an average

length of 255 nm and diameter of 4 nm. Li et al. (2012) used a high-pressure homogenizer with an ionic liquid pretreatment to produce nanocellulose from bagasse. Their results indicated that the nanocellulose preparation process was optimized after 30 cycles of passing through the homogenizer while the nanocellulose diameter ranged between 10 and 20 nm with particle morphologies exhibiting lower flexibility, strength, and aspect ratio as compared to CNF (Siqueira et al. 2010). Hassan et al. (2012) used an ultrafine grinder and a high-pressure homogenizer to extract bagasse CNF. Their results indicated that fibrillation was achieved after almost 30 passes through the ultrafine grinder when the dimensions of the refined pulp reached the nanosize range. However, they observed no significant changes in the diameter of the CNF because most fibrillation, after almost 30 passes, took place by using ultrafine grinding process. Soda pulping is the most common process in the preparation of non-wood pulps. In addition, the presence of anthraquinone (AQ) in the pulping process increases the rate of delignification and decreases the rate of carbohydrate degradation by blocking their active groups and reducing the rate of oxidation (Biermann 1996). On the other hand, because of the removal of the non-cellulosic constituents and destruction of the hydrogen bonds between cellulose chains, during the alkali delignification (Mantanis et al. 1995), it is reasonable to develop an alkali delignification pulping process as a critical and initial step before isolating the cellulose nanofibers and nanocrystals (Dufresne 2012). Moreover, nowadays, the conversion of biomass into chemicals and energy is vital for sustaining life (Amidon and Liu 2009), and bio-refinery is known as an important process for using renewable resources instead of fossil fuels in order to prepare commodity products, liquid fuels, and electricity. This process in pulp and paper industry is identified by using sulfur-free treatment for isolating hemicellulose before pulping process (Bajpai 2013). In this study, hot water extraction as a suitable bio-refinery process has been used before pulping stage.

To the best of the authors' knowledge, no published work has been reported on the isolation of bagasse CNF using an optimized alkali delignification approach. The main objective of the present work was to develop a sulfur-free and bio-refinery chemo-mechanical treatment which is known as a suitable procedure to extract high content of α-cellulose (Andrade and Colodette 2014) for isolating CNF from bagasse. The most important alkali pulping parameters—alkali concentration and cooking temperature—were optimized using the response surface method. To obtain a high degree of fibrillation, water retention value (WRV), Kappa number, α-cellulose, and hemicellulose were selected as model responses. Morphological changes during the chemical treatments were tracked by SEM and OM. In addition, the size and morphological characteristics of the CNF were studied by DLS and TEM. The chemical compositions and chemo-physical properties were analyzed using the NREL procedure and FTIR, respectively. Moreover, XRD was employed to study the variations in cellulose crystallinity during the chemo-mechanical treatments.

## Experimental

### Materials

Bagasse was obtained from a local sugar production plant (MirzaKuchak Khan Co, Khuzestan, Iran) and used as a source of cellulose. It had been air-dried and crushed into lengths of 2–3 cm by a hammer mill.

### Cellulose nanofibrils (CNF) extraction

#### Depithing and de-waxing

The depithing process was performed in two stages: (1) dry depithing by screening, and (2) moist depithing using a disintegrator for 30 min. In order to obtain a high-quality depithed bagasse pulp, non-structural materials and extractives were removed during 24 h in a Soxhlet apparatus using water and ethanol (Sluiter et al. 2005b).

#### Autohydrolysis and alkali pulping

Prior to pulping, the hemicellulose and remaining piths were removed with hot water, known as a sulfur-free and bio-refinery process, via autohydrolysis in a 500-mL stainless steel high-pressure reactor, which had its temperature set by an oil bath (Amiri et al. 2010). The optimal conditions of autohydrolysis were set as recommended in Hamzeh et al. (2013). Briefly, bagasse fibers and deionized water were added to the reactor based on the weight of oven-dried fibers in solid-to-liquor ratio of 1:8 (w/w). Maximum autohydrolysis temperature was set at 170 °C, and this temperature was achieved after 90 min with 10-min holding time at the maximum temperature. For delignification, the hydrolyzed bagasse was pulped by the same reactor at a solid-to-liquor ratio of 1:4 (w/w) and different cooking conditions. The maximum cooking temperature was set to 150 °C, reached in 60 min (Agnihotri et al. 2010). After each pulping cycle, the reactor was immediately dipped in ice water. Then, the residual fibers and liquor were separated on a 200 mesh before the residual was washed with warm distilled water. The conditions of the autohydrolysis and pulping processes are presented in Table 1.

**Table 1** Autohydrolysis and pulping conditions of depithed bagasse

|  | Autohydrolysis | Pulping treatment |
| --- | --- | --- |
| NaOH concentration (wt%) | 0 | 10–17.5 |
| Solid-to-liquor ratio | 1:8 | 1:4 |
| Maximum temperature (°C) | 170 | 150 |
| Time to reach maximum temperature (min) | 90 | 60 |
| Time at maximum temperature (min) | 10 | 0–60 |

*Optimization of pulping*

Pulping conditions were optimized based on a rotatable central composite design (RCCD) using the Design-Expert software (version 8.0.7.1). According to Agnihotri et al. (2010), the factors with the greatest effects were (a) alkali concentration (10–17.5 wt%) and (b) pulping time (0–60 min). Kappa number ($R_1$), WRV ($R_2$), α-cellulose ($R_3$), and hemicellulose ($R_4$) were chosen as model responses. Analysis of variance (ANOVA) was carried out to select the optimum conditions (Table 2).

*Elemental chlorine-free (ECF) bleaching conditions*

The insoluble residual lignin was isolated by ECF bleaching in three steps based on the method described by Jonoobi et al. (2009). In the first step ($D_1$), sodium chlorite ($NaClO_2$) with equivalent chlorine of 0.73 was added to acetic acid in order to release chlorine dioxide ($ClO_2$) as a bleaching agent. In the second step, hydrogen peroxide ($H_2O_2$) with the equivalent chlorine of 2.09 was used in the presence of sodium hydroxide so that it could boost delignification by generating perhydroxyl anion as a nucleophilic bleaching agent (EP). In the last step ($D_2$), the pulp was bleached again with sodium chlorite and acetic acid to remove the residual lignin from the surface of the fibers. Prior to the bleaching experiments, the Kappa number of pulp was measured as a parameter to determine the amount of chlorine required for bleaching (Biermann 1996). In addition, Kappa factor known as an important number in pulp industry in order to calculate the required amount of oxidant in bleaching processes ranged between 0 and 0.25. By increasing Kappa number, more brightness and less bleaching stages are expected to be obtained (Chai and Zhu

**Table 2** Pulping process parameters and experimental design factors and responses

| Run | $A^a$ | $B^a$ | $R_1$ | $R_2$ | $R_3$ | $R_4$ |
|---|---|---|---|---|---|---|
| 1 | 10 (−1) | 10 (−1) | 29.79 | 198.84 | 82.34 | 13.51 |
| 2 | 0 (−1.41) | 13.75 (0) | 25.11 | 220.44 | 83.54 | 12.53 |
| 3 | 60 (0) | 17.5 (0) | 18.74 | 266.56 | 87.88 | 9.12 |
| 4 | 35 (0) | 19.04 (1.41) | 18.76 | 265.71 | 87.71 | 9.5 |
| 5 | 35 (0) | 13.75 (0) | 27.02 | 229.65 | 84.87 | 10.16 |
| 6 | 70.25 (1.41) | 13.75 (0) | 19.05 | 254.07 | 86.68 | 10.64 |
| 7 | 35 (0) | 13.75 (0) | 26.49 | 230.26 | 84.91 | 11.43 |
| 8 | 35 (0) | 8.46 (−1.41) | 28.98 | 201.35 | 82.04 | 14.41 |
| 9 | 35 (0) | 13.75 (0) | 26.03 | 230.48 | 85.05 | 11.35 |
| 10 | 35 (0) | 13.75 (0) | 27.77 | 229.72 | 84.97 | 10.77 |
| 11 | 60 (1) | 10 (−1) | 23.47 | 226.97 | 84.88 | 11.05 |
| 12 | 10 (−1) | 17.5 (1) | 18.81 | 248.51 | 86.77 | 9.02 |
| 13 | 35 (0) | 13.75 (0) | 27.99 | 229.56 | 85.81 | 10.92 |

$A$, $B$, $R_1$, $R_2$, $R_3$, and $R_4$ are time (min), alkali concentration (%), Kappa number, WRV (%), α-cellulose (%), and hemicellulose content (%)

[a] The numbers in parentheses indicate coded values

**Table 3** Bleaching conditions

|  | $D_1$ | $E_P$ | $D_2$ |
| --- | --- | --- | --- |
| Reagent (wt%) | NaClO$_2$ (2) | H$_2$O$_2$ (1) | NaClO$_2$ (1.25) |
|  | CH$_3$COOH (3) | NaOH (1.5) | CH$_3$COOH (3) |
| Pulp consistency (wt%) | 10 | 10 | 10 |
| Temperature (°C) | 60 | 70 | 80 |
| Time (min) | 60 | 90 | 120 |
| pH | 4.1 | 10.5 | 4.1 |

1999). In this study, Kappa factor is considered to be 0.25. The conditions used in the bleaching steps are summarized in Table 3.

*Fibrillation conditions*

For isolating CNF, bleached pulp which had never been dried before was refined using a laboratory PFI mill with a treatment level of 25,000 revolutions. The water slurry with 1 wt% of the refined fibers was then passed two times through an ultrafine grinder (MKCA6-3; Masuko Sangyo Co., Ltd., Japan) at 1500 rpm to obtain hydrocolloid slurries of the CNF. Eventually, several droplets of chloroform were added into the slurry and stored in the refrigerator at 4 °C.

# Characterization

## Chemical characterization

Fiber components (i.e., extractives, carbohydrates, and lignin) were determined based on the standard procedures recommended by the National Renewable Energy Laboratory, NREL (Sluiter et al. 2005a, b). Furthermore, the ASTM (D1103-60 and D1104-56) procedures were used to determine the α-cellulose and hemicellulose contents of the bagasse pulp for the optimization of the delignification pulping process. Kappa number was calculated according to Chai and Zhu's procedure under strong acidic conditions (Chai and Zhu 1999).

## Water retention value (WRV)

The samples were submerged in distilled water, and the wet bagasse pulp was centrifuged at 4500 gravity and 20 °C for 20 min. The pulp was then dried at 105 °C for 3 h. The value for WRV was determined using Eq. (1) below:

$$WRV\,(\%) = (W_w - W_d)/W_d \times 100 \tag{1}$$

where $W_w$ is the pulp weight after centrifugation and $W_d$ is the pulp weight after drying (Saito et al. 2007).

## Microscopic observations

Optical microscopy (OM) was used to evaluate the morphology and dimensions of pulped bagasse samples after each of the various pulping conditions. In addition, scanning electron microscopy, SEM (Zeiss, 1450EP, Germany), was employed to investigate fiber morphology before and after chemical treatments. For this purpose, a sheet of each sample was coated with gold in a vacuum coater to avoid charging. The sample was then observed under SEM operating at 8.5 and 17.5 kV. The final CNF morphology was studied by transition electron microscopy, TEM (Zeiss, EM10C-80 kV, Germany). A quantity of 5 μL of the CNF suspension with a solid content of about 0.001 wt% was well dispersed in ethanol using the ultrasonic process (Misonix- S3000 USA) before it was cast on a holey carbon-coated grid and the excess water was absorbed by a filter paper. Microscopic images were analyzed by an image analyzer program (UTHSCSA Image Tool, Dental Diagnostic Science, 2002).

## Dynamic light scattering (DLS)

DLS was used to measure the size distribution of CNF in a water slurry (0.1 wt%). This measurement was taken with a detection angle of 173° at 25 °C using a 4-mW He–Ne laser operating at a wavelength of 633 nm. DLS results predict the peak intensity of size distributions of the CNF suspension by assuming a spherical structure for the cellulose chains. This analysis is based on the correlation functions calculated by Multiple Narrow Modes algorithm in the instrument's software.

## Fourier transform infrared (FTIR) spectroscopy

FTIR spectroscopy was used to determine possible changes in the chemical composition and functional groups before and after the chemical treatments. Dried samples were ground into powder, blended with potassium bromide (KBr), and pressed into a thin pellet. The FTIR spectra of each sample were scanned within a range of 500–4000 cm$^{-1}$.

## X-ray diffraction (XRD)

X-ray diffraction (X'Pert, Philips, Germany) was carried out to evaluate the crystallinity of the fibers after chemical and mechanical treatments using Cu Kα radiation ($\lambda = 0.15418$ nm) at 40 kV and 30 mA in the range of $2\theta = 10°$–50°. Equation (2) below was used to calculate the crystallinity index of cellulose ($C_I$):

$$C_{I(\%)} = (I_{200} - I_{am})/I_{200} \times 100 \qquad (2)$$

where $I_{200}$ and $I_{am}$ represent the crystalline regions of cellulose $I$ and the amorphous regions at $2\theta$ of about 22.5° and 18°, respectively.

# Results and discussion

## Optimization of alkali pulping conditions

The three stages of initial, bulk, and residual delignification have been found to take place during the pulping process. Moreover, a critical temperature has also been identified for the thermoplastic behavior of lignin, at which delignification process happens significantly (Kim and Holtzapple 2006). For bagasse, bulk delignification was completed at 150 °C; thus, it will not be economically justified to increase temperature beyond this. On the other hand, increasing the cooking temperature above 150 °C for pulped bagasse leads to peeling, de-polymerization, and secondary peeling reactions (Agnihotri et al. 2010). In this study, the effect of temperature on pulping was assumed to be constant, and thus, the experiment was designed such that the pulping process conditions could be optimized based on a rotatable central composite design. Statistical ANOVA was used to determine the significance and adequacy of the model equations and terms. Table 4 summarizes some of the response properties obtained from ANOVA.

"Probe $> F$" value less than 0.050 for a factor indicates its significance in the model. Here, for all model responses ($R_1$, $R_2$, $R_3$, and $R_4$), the values are very small ($<0.05$). The final responses predicted by the model were obtained and presented in Eqs. (3–6) in coded form as follows:

For Kappa number ($R_1$):

$$R_1 = 27.06 - 1.87A - 3.77B + 1.56AB - 2.56A^2 - 1.66B^2 \tag{3}$$

For WRV ($R_2$):

$$R_2 = 229.93 + 11.72A + 22.53B - 2.52AB + 3.62A^2 + 1.75B^2 \tag{4}$$

For α-cellulose ($R_3$):

$$R_3 = 85.19 + 1.01A + 1.93B \tag{5}$$

For hemicellulose ($R_4$):

$$R_4 = 11.11 - 0.63A - 1.67B \tag{6}$$

**Table 4** Some response properties from ANOVA tables

| Response | Name | Unit | Minimum | Maximum | Model | $F$ value | Probe $> F$ | Lack of fit |
|---|---|---|---|---|---|---|---|---|
| $R_1$ | Kappa number | – | 18.74 | 29.79 | Quadratic | 79.35 | 0.0001 | 0.45 |
| $R_2$ | WRV | % | 198.84 | 266.56 | Quadratic | 5464.89 | 0.0001 | 1.36 |
| $R_3$ | α-cellulose | % | 82.04 | 87.88 | Linear | 106.48 | 0.0001 | 1.28 |
| $R_3$ | Hemicellulose | % | 9.02 | 14.41 | Linear | 23.03 | 0.0002 | 2.86 |

**Table 5** Statistical parameters from ANOVA tables

|  | Kappa number | WRV | α-cellulose | Hemicellulose |
|---|---|---|---|---|
| SD | 0.73 | 0.44 | 0.42 | 0.74 |
| Mean | 26.46 | 233.34 | 85.19 | 11.11 |
| C.V. % | 2.97 | 0.19 | 0.5 | 6.7 |
| PRESS | 10.99 | 5.91 | 3.29 | 10.97 |
| $R^2$ | 0.9827 | 0.9997 | 0.9551 | 0.8216 |
| $R^2_{adj}$ | 0.9703 | 0.9996 | 0.9462 | 0.7859 |
| $(R^2_{pre})$ | 0.9484 | 0.9989 | 0.9174 | 0.6459 |
| Adeq precision | 23.578 | 229.195 | 28.994 | 13.22 |

The important statistical parameters of these models are presented in Table 5. As can be seen, both the standard deviation and the coefficient of variation (C.V. %), defined as the residual variation in the data relative to the size of the mean, are relatively low and the results are, therefore, reliable (Satari Baboukani et al. 2012).

In addition, coefficients of determination ($R^2$), defined as the amount of variation around the mean, were 98.3, 99.9, 95.5, and 82.2 % for Kappa number, WRV, α-cellulose, and hemicellulose, respectively (Satari Baboukani et al. 2012). On the other hand, the value for the adjusted coefficients of determination ($R^2_{adj}$), defined as the amount of variation around the mean, explained by the model, and adjusted for the number of terms in the model, indicates the high significance of the models. As can be seen in Table 5, there are other important parameters such as coefficient of determination ($R^2_{pre}$) and adequate precision which determine whether or not model precision is adequate (Satari Baboukani et al. 2012). These model parameters indicated that the accuracy of the applied model was acceptable. Figure 1 shows the effects of pulping conditions (alkali concentration and pulping time) on different responses in three-dimensional surface plots. All the responses are clearly mapped based on the above equations against the experimental factors and, based on polynomial analyses, they are presented in two quadratic models for Kappa number and WRV as well as two linear models for α-cellulose and hemicellulose.

Figure 1a provides the details of the Kappa number in comparison with the experimental factors. Evidently, the Kappa number ranging from 18.74 in the run of three (pulping time 60 h and alkali concentration 17.5 %) to 29.74 in the run of one (pulping time 10 h and alkali concentration 10 %) decreased drastically after delignification; this decrease is due to the removal of high lignin percentage values, which can improve upon the mechanical defibrillation process in the subsequent steps. The minimum value was obtained for pulping with an alkali concentration of 17.5 wt% for 1 h. WRV represents the ability of fibers to uptake water and swell. Indeed, WRV has direct relationships with the bonding ability of the fibers, the exposed cellulose surface area, and the degree of fibrillation of CNF (Cheng et al. 2011; Dufresne 2012). Figure 1b compares the values of WRV against the experimental factors. Based on Fig. 1b, higher values of WRV were obtained for lower values of residual lignin in cell walls; this must have been due to the opening
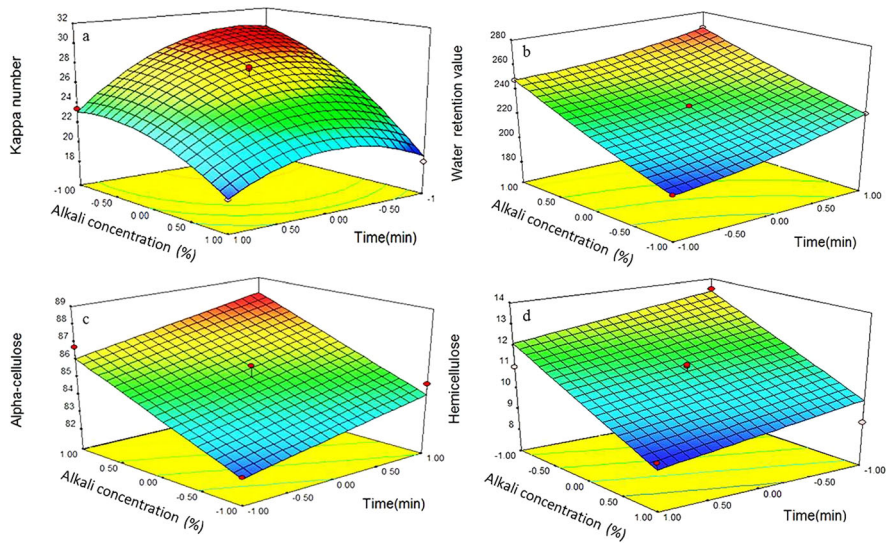
**Fig. 1** Three-dimensional (3D) response surface for **a** Kappa number, **b** WRV, **c** α-cellulose, and **d** hemicellulose as a function of time and alkali concentration

of fiber bundles that exposed more cellulose to absorb water (Dufresne 2012). Similar to the Kappa number, the highest WRV value was obtained for pulping with an alkali concentration of 17.5 wt% for 1 h. Figure 1c, d shows the variations in α-cellulose and hemicellulose contents against the experimental factors, respectively. The preparation of high α-cellulose content from bagasse pulp was an essential step for producing CNF. In addition, the stability of final CNF suspension will be improved in the presence of the hemicelluloses remaining on the surface of CNF (Dufresne 2012); moreover, a low percentage of hemicellulose facilitates the isolation of microfibril from plant cell wall during the mechanical treatments and enhances the CNF production yield. In this case, the fibrillation yield of bagasse fibers was found to be about 99 % under the optimized conditions based on a procedure by Alila et al. (2013). The ratio of hemicellulose to α-cellulose is another important parameter for the preparation of cellulose pulp by promoting the swelling of microfibers (Casey 1952). In this work, the hemicellulose/α-cellulose ratio was found to be 0.102 which was acceptable for starting CNF isolation. Based on the experimental design, the optimum conditions for the alkali pulping process were determined to include an alkali concentration of 17.5 wt% and a pulping time of 1 h for which the values for the Kappa number, WRV, α-cellulose, and hemicellulose would be 18.7, 267.0 (%), 88.1 (%), and 8.8 (%), respectively.

## Chemical composition

In this study, piths and extractives were removed prior to the pulping process, and this can enhance the liquor penetration into the bulk fibers as well as reduce the pith-associated problems (Casey 1952; Zhang et al. 2013). The clean, depithed bagasse

Table 6 Chemical composition of the raw and chemically treated bagasse pulps

| Components and parameters | Untreated | Hydrolyzed | Pulped | Bleached |
|---|---|---|---|---|
| Glucan | 42.2 | 57.26 | 88.23 | 91.8 |
| Xylan | 21.8 | 10.96 | 8.82 | 7.38 |
| Galactan | 0.6 | 0 | 0 | 0 |
| Mannan | 0 | 0 | 0 | 0 |
| Arabinan | 1.8 | 0.27 | 0 | 0 |
| Total lignin | 23.5 | 28.9 | 2.95 | 0.82 |
| Extractives | 10.1 | 2.61 | 0 | 0 |
| $\alpha$-cellulose | – | – | 87.88 | 90.2 |
| Kappa number | – | – | 18.74 | 6.5 |

was then subjected to the steps of autohydrolysis, alkali pulping, and bleaching. The chemical compositions of the raw and chemically treated bagasse fibers are presented in Table 6.

The extractive-free and depithed bagasse fibers were prepared for autohydrolysis treatment prior to the pulping process. Hot water autohydrolysis was used as a selective treatment to remove hemicellulose with minimum degradation of the cellulose chains. During the autohydrolysis process, acetic acid is generated due to the release of the acetyl groups present in the hemicellulose structure, and pH is, therefore, reduced to around 3–4 (Andrade and Colodette 2014; Borrega et al. 2013; Hamzeh et al. 2013; Lei et al. 2010). In this condition, hemicellulose is dissolved to oligomer fragments and subsequently hydrolyzed to sugar monomers and other products such as hydroxyl methylfurfural (HMF) from hexose and furfural from pentose and uranic acid (Andrade and Colodette 2014). In this work, xylan, the main hemicellulosic compound of bagasse (Andrade and Colodette 2014), decreased after autohydrolysis from 21.8 to 10.96 wt% (Table 6). The final pH reached 3.3, and the autohydrolysis yield was 73 wt%. Once the autohydrolysis process is complete, lignin fragments migrate to the surface of the bagasse pulp, resulting in faster delignification and, therefore, in reduced values of total pulp yield and Kappa number. The same trend has also been observed in previous studies (Hamzeh et al. 2013).

In order to obtain a suitable pulp for CNF preparation, an optimized soda-AQ pulping process was carried out to achieve values of 34 wt% and 18.74 for the final pulp yield and the Kappa number, respectively. The lignin content of the final pulp was 2.95 wt%, which indicates the removal of almost all the lignin. In addition, the hemicellulosic carbohydrates of xylan, arabinan, and galactan reduced to 8.82, 0, and 0 wt%, respectively. In the bleaching sequence, perhydroxyl ions were used in the $E_p$ stage to oxidize the remaining lignin structures (Bajpai 2012). Moreover, the $D_1$ and $D_2$ bleaching stages were performed to produce a high-quality bleached pulp by removing the residual phenolic molecules such as lignin, polyphenol, and proteins by sodium chlorite (Dufresne 2012). This resulted in almost complete removal of the lignin content, while the $\alpha$-cellulose and glucan contents reached 90.2 and 91.8 %, respectively.

## Morphological analysis

As can be seen in Fig. 2, the middle lamella was drastically destroyed and individual fibers were isolated from the plant cell walls under all conditions after the pulping process was over; however, some fiber bundles were still present. Image analysis showed that the obtained bagasse microfibers pulped by 17.5 wt% sodium hydroxide for 1 h had more individual thin microfibers than the other microfibers obtained under other alkali conditions. This confirms the results obtained under optimized pulping conditions in the experimental design.

Furthermore, for closer scrutiny, the morphology of bagasse microfibers chemically treated at different stages was analyzed by SEM images (Figs. 3, 4). It is clear from Figs. 3a and 4a that the raw bagasse fibers were linked together by lignin and packed with strong bonding interactions. Based on image analysis, the average diameter and range of the raw bagasse fibers were $276 \pm 1$ and 200–600 μm (Fig. 3c). It can be seen that bagasse fibers were not homogeneous in diameter, and similar result was reported by Premjai et al. (2014).
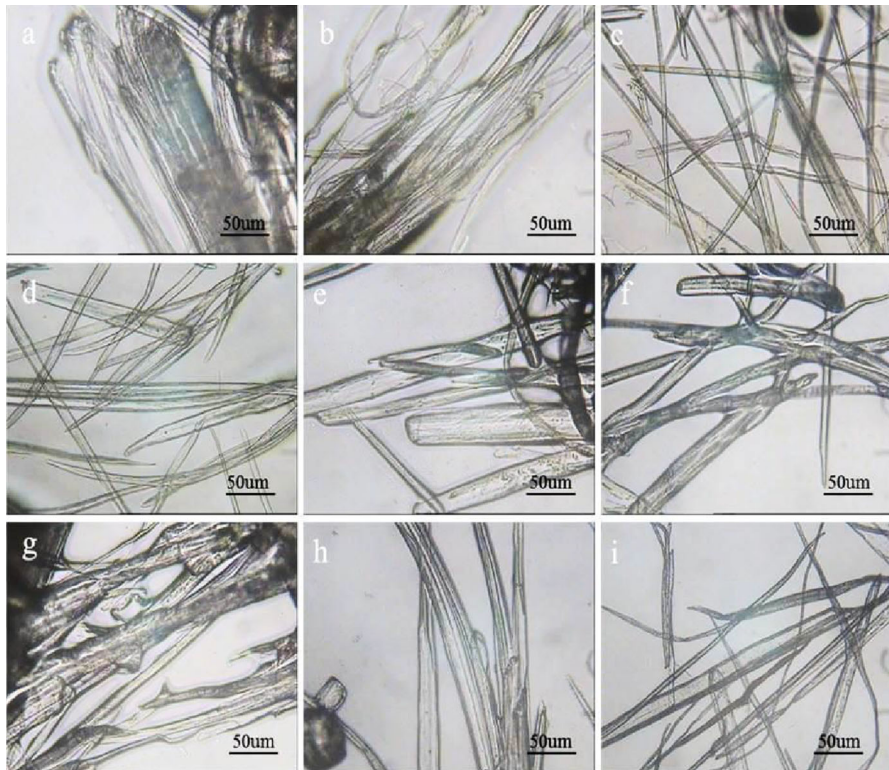


**Fig. 2** Optical micrograph of bagasse structure after alkali treatment for **a** run 1 (A:10, B:10); **b** run 2 (A:0, B:13.75); **c** run 3 (A:60, B:17.5); **d** run 4 (A:35, B:19.04); **e** run 5 (A:35, B:13.75); **f** run 6 (A:70.25, B:13.75); **g** run 8 (A:35, B:8.46); **h** run 11 (A:60, B:10); and **i** run 12 (A:10, B:17.5)
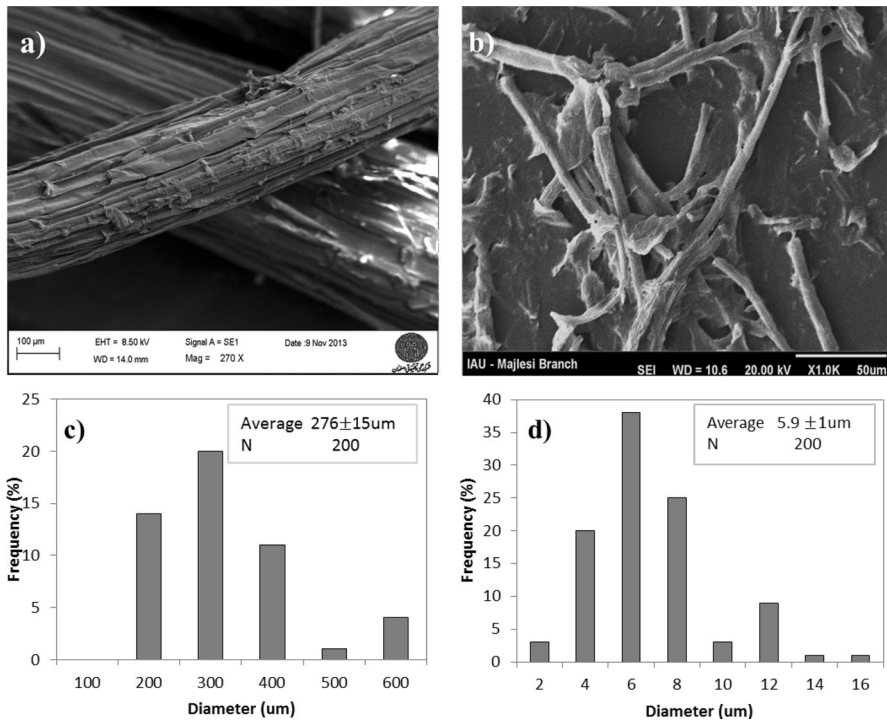
Fig. 3 SEM images: **a** untreated bagasse fibers, **b** pulped bagasse fibers after run 3, **c** diameter distribution of untreated fibers, **d** diameter distribution of treated fibers

Figure 4b depicts the autohydrolyzed fibers. Clearly, fiber diameter did not change as a result of autohydrolysis, but its smoothness was enhanced, probably due to the migration of depolymerized lignin fragments to the surface. As can be seen in Figs. 3b and 4c, lignin was drastically removed after the pulping process and individual microfibers were isolated. Image analysis showed that the diameter of the raw bagasse pulp decreased from 200 to 600 μm (Fig. 3c) to 2–16 μm (Fig. 3d) as a result of alkali pulping under optimized conditions such that more than 81 % of the pulped bagasse had a diameter below 8 μm. However, a small amount of the residual lignin fragments remained stocked on the surface of the microfibers. Eventually, this residual lignin was also removed after the bleaching process and a smooth surface was obtained. Image analysis revealed an average microfiber diameter of 5.9 ± 1 μm, which is reasonably acceptable for starting the final pulp fibrillation. CNF are located within fiber bundles by strong hydrogen bonding (Dufresne 2012).

The isolation of highly crystalline and defect-free CNF, therefore, requires the association energy between cellulose chains to be destroyed. In this study, CNF isolation was carried out in two stages using a PFI mill refiner and an ultrafine grinder. Figure 5a shows the morphology of the refined and bleached pulp. Evidently, although the fibril/fiber ratio greatly increased and the fibrillation was
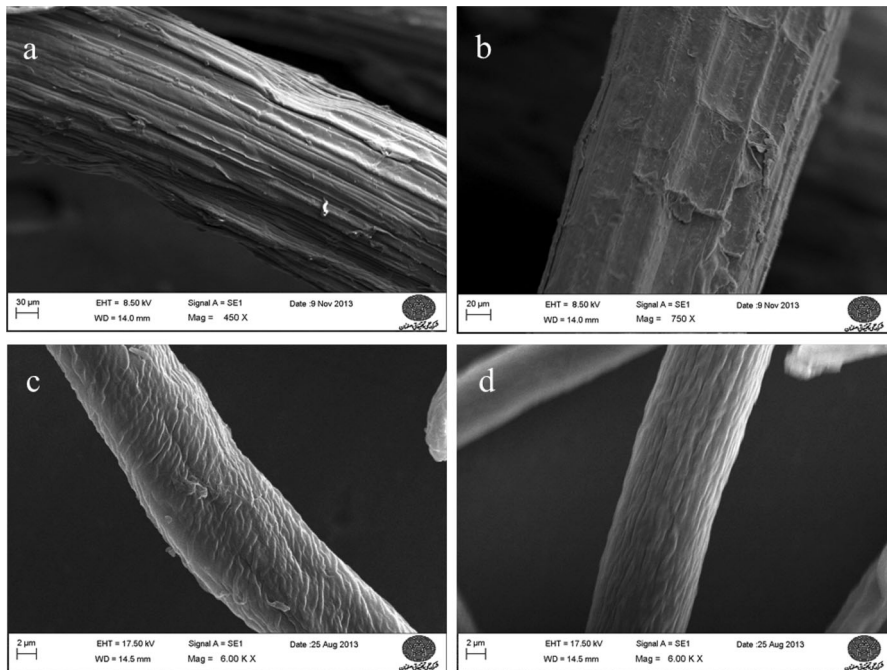
**Fig. 4** SEM images of depithed bagasse structure: **a** raw fibers, **b** autohydrolyzed fibers, **c** pulped fibers, and **d** bleached fibers

improved, only the weak microfibril bonds that need a lower energy for defibrillation in the primary cell walls were isolated, leading to only partial defibrillation (Ferrer et al. 2012a, b). An ultrafine grinder was, therefore, used in a second stage to produce CNF with a high level of fibrillation. The visual observation of the TEM images reveals that a web-like network structure with a high fibril density and complex orientation and distribution emerged after ultrafine grinding (Fig. 5b) (Ferrer et al. 2012a). Further image analysis (Fig. 5c) showed that the average diameter of the CNF thus produced reached $11.13 \pm 1$ nm, which is completely in the nanosize range with lengths being in the micrometer scale. Therefore, compared to the mechanical process optimization (Hassan et al. 2012; Li et al. 2012), an optimized chemical process followed by double passing through the ultrafine grinder was found to be completely effective in isolating the final CNF with a suitable diameter.

The DLS results in Fig. 5d indicate that the hydrodynamic diameters of the diluted CNF had a single peak at around 860 nm, which was related to the average size of the CNF agglomerates and shows its micelles orientation in the fluid. These results obtained here are similar to those obtained from a pilot CNF oxidizing process using the 2,2,6,6-tetramethylpiperidine-1-oxyl radical (TEMPO) catalyst (Dimic-Misic et al. 2013). The optimized alkali conditions can be thus successfully used for preparing the nanofibrillated bagasse.
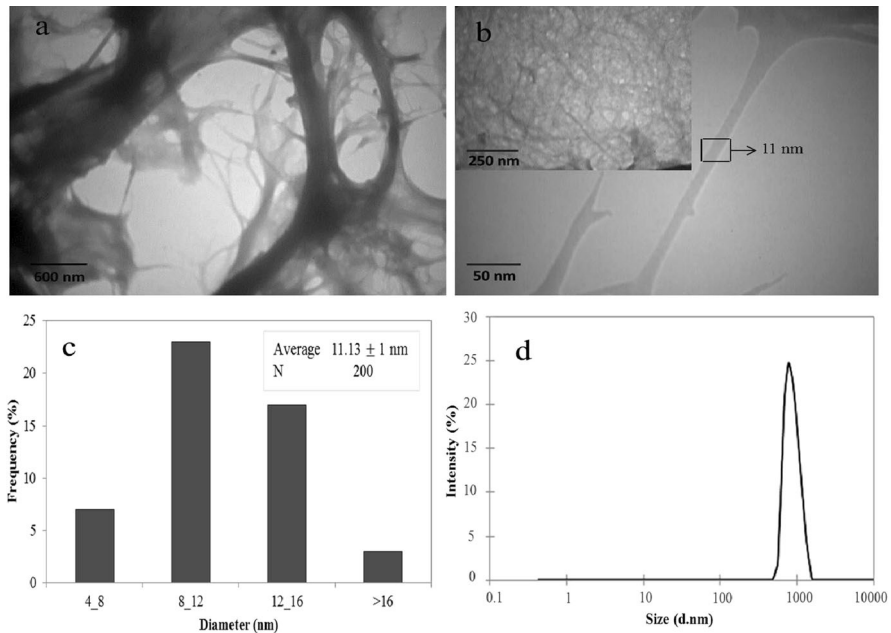
**Fig. 5** Transition electron micrographs **a** refined fibers after 25,000 revolutions through PFI mill, **b** CNFs after two passes of ultrafine grinder, **c** size distributions of ground CNF, and **d** size distributions of CNF aggregates by DLS analysis in a water medium

## FTIR analysis

FTIR analysis was employed to trace the changes in the functional groups of the bagasse pulp during chemical treatments. The spectra of the raw, autohydrolyzed, pulped, and bleached bagasse samples are presented in Fig. 6. The dominant peaks around 3426 and 2900 cm$^{-1}$ belonged to the stretching vibrations of OH and CH of the $CH_2$ and $CH_3$ groups, respectively (Viera et al. 2007). The raw bagasse sample had its main peaks between 700 and 2000 cm$^{-1}$, which are mostly related to lignin and hemicellulose. The absorbance peaks at 1730 and 1634 cm$^{-1}$ were attributed to the C=O stretching of the acetyl or carboxylic acid and the carbonyl with an aromatic ring, respectively. In addition, the transmittance peaks at 1620–1595 cm$^{-1}$ are responsible for the stretching of the aromatic ring of the lignin structure. It was also found that the most important peaks for the delignification process were located at 1512 and 1250 cm$^{-1}$, which were related to the C=C stretching of the aromatic ring and the C–O stretching of the ether linkage, respectively. Upon chemical pretreatment, these peaks almost vanished, indicating the significant removal of lignin and hemicellulose during the chemical treatments (Rosa et al. 2010; Viera et al. 2007).

The peaks at 896, 1062, and 1166 cm$^{-1}$, respectively, were assigned to the functional groups in b-glucosidic linkages between the sugar units, C–O symmetric stretching of primary alcohol, and C–O–C antisymmetric bridge stretching
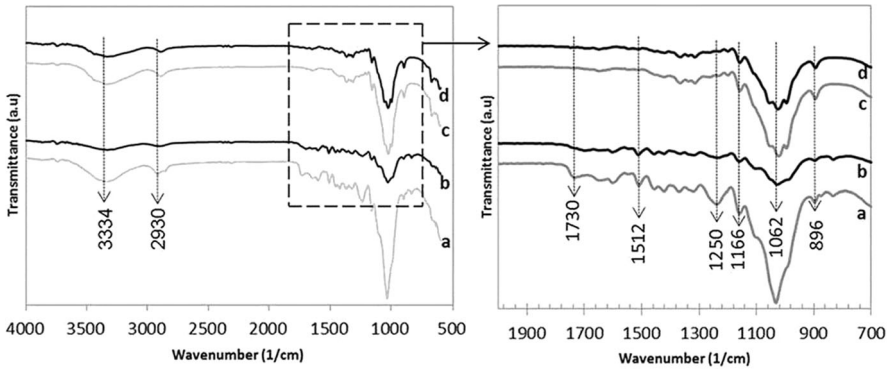
**Fig. 6** FTIR spectra **a** depithed bagasse, **b** autohydrolyzed bagasse, **c** pulped bagasse, and **d** bleached bagasse

(Alemdar and Sain 2008). These peaks appeared after chemical treatment. Based on the FTIR spectra, pretreatment was effective in removing the main portion of the non-cellulosic components.

### X-ray diffraction analysis

The crystallinity index is a factor involved in the thermomechanical properties of nanocellulose (Chen et al. 2011). XRD analysis was used to calculate the values for the crystalline indices of the untreated as well as the chemically and the mechanically treated bagasse fibers as 45.81, 63.12, and 58.21 %, respectively (Fig. 7). An increase of about 20 % was observed in the crystallinity of CNF as a result of removing lignin and hemicellulose during the chemical treatment steps. A slight decrease was, however, observed in this index with the mechanical treatment, which can be attributed to peeling-off effect of the cellulose chains on the surface of the crystallites (Alila et al. 2013).
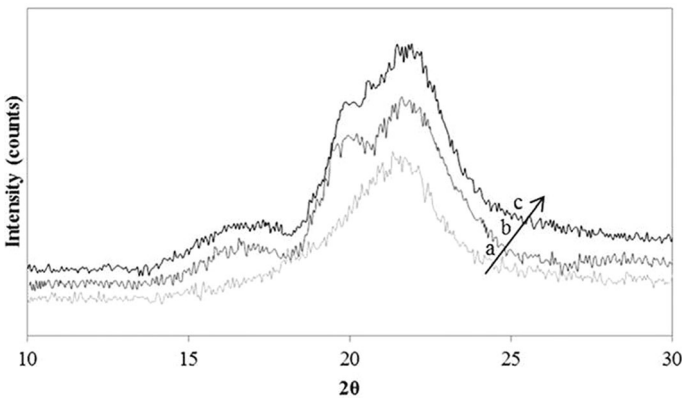


**Fig. 7** X-ray diffraction patterns of **a** untreated, **b** chemically treated, and **c** mechanically treated fibers

# Conclusion

Highly nanofibrillated bagasse was successfully extracted via modified chemo-mechanical method. The optimized conditions of delignification were obtained for 1 h at 150 °C with an alkali concentration of 17.5 wt%. TEM and DLS results showed that the average diameter of the CNF was in nanometer range. Moreover, chemical analysis and Kappa number determination revealed that the high hemicellulose and lignin removals after chemical treatment led to a high α-cellulose content. In addition, FTIR confirmed the successful removal of lignin and hemicellulose from the bagasse structure. XRD analysis revealed a higher crystallinity of the chemo-mechanically treated bagasse samples. The proposed process can be effectively exploited to produce CNF with properties suitable for nanocomposite preparations from bagasse.

# References

Agnihotri S, Dutt D, Tyagi C (2010) Complete characterization of bagasse early species of saccharum officinarum-CO 89003 for pulp and paper making. BioResources 5:1197–1214

Alemdar A, Sain M (2008) Isolation and characterization of nanofibers from agricultural residues—wheat straw and soy hulls. Bioresour Technol 99:1664–1671

Alila S, Besbes I, Vilar MR, Mutjé P, Boufi S (2013) Non-woody plants as raw materials for production of microfibrillated cellulose (MFC): a comparative study. Ind Crops Prod 41:250–259

Amidon TE, Liu S (2009) Water-based woody biorefinery. Biotechnol Adv 27:542–550

Amiri H, Karimi K, Roodpeyma S (2010) Production of furans from rice straw by single-phase and biphasic systems. Carbohydr Res 345:2133–2138

Andrade MF, Colodette JL (2014) Dissolving pulp production from sugar cane bagasse. Ind Crops Prod 52:58–64

Bajpai P (2012) Environmentally benign approaches for pulp bleaching. Elsevier, Amsterdam

Bajpai P (2013) Biorefinery in the pulp and paper industry. Elsevier, Amsterdam

Biermann CJ (1996) Handbook of pulping and papermaking. Academic press, San Diego

Borrega M, Tolonen LK, Bardot F, Testova L, Sixta H (2013) Potential of hot water extraction of birch wood to produce high-purity dissolving pulp after alkaline pulping. Bioresour Technol 135:665–671

Casey JP (1952) Pulp and paper. Chemistry and chemical technology. Interscience, New York

Chai X-S, Zhu Y (1999) Rapid pulp Kappa number determination using spectrophotometry. Institute of Paper Science and Technology. http://hdl.handle.net/1853/3065. Accessed July 2015

Chen W, Yu H, Liu Y, Chen P, Zhang M, Hai Y (2011) Individualization of cellulose nanofibers from wood using high-intensity ultrasonication combined with chemical pretreatments. Carbohydr Polym 83:1804–1811

Cheng Q, De Vallance D, Wang J, Wang S (2011) Advanced cellulosic nanocomposites materials. In: Advances in composite materials. INTECH, West Virginia

Dimic-Misic K, Puisto A, Gane P, Nieminen K, Alava M, Paltakari J, Maloney T (2013) The role of MFC/NFC swelling in the rheological behavior and dewatering of high consistency furnishes. Cellulose 20:2847–2861

Dufresne A (2012) Nanocellulose: from nature to high performance tailored materials. Walter de Gruyter, Berlin

Dufresne A (2013) Nanocellulose: a new ageless bionanomaterial. Mater Today 16:220–227

Ferrer A, Filpponen I, Rodríguez A, Laine J, Rojas OJ (2012a) Valorization of residual Empty Palm Fruit Bunch Fibers (EPFBF) by microfluidization: production of nanofibrillated cellulose and EPFBF nanopaper. Bioresour Technol 125:249–255

Ferrer A et al (2012b) Effect of residual lignin and heteropolysaccharides in nanofibrillar cellulose and nanopaper from wood fibers. Cellulose 19:2179–2193

Hamzeh Y, Ashori A, Khorasani Z, Abdulkhani A, Abyaz A (2013) Pre-extraction of hemicelluloses from bagasse fibers: effects of dry-strength additives on paper properties. Ind Crops Prod 43:365–371

Hassan ML, Mathew AP, Hassan EA, El-Wakil NA, Oksman K (2012) Nanofibers from bagasse and rice straw: process optimization and properties. Wood Sci Technol 46:193–205

Jonoobi M, Niska KO, Harun J, Misra M (2009) Chemical composition, crystallinity, and thermal degradation of bleached and unbleached kenaf bast (*Hibiscus cannabinus*) pulp and nanofibers. BioResources 4:626–639

Kalia S, Kaith B, Kaur I (2011) Cellulose fibers: bio-and nano-polymer composites. Green chemistry and technology. Springer, Heidelberg

Kim S, Holtzapple MT (2006) Delignification kinetics of corn stover in lime pretreatment. Bioresour Technol 97:778–785

Lei Y, Liu S, Li J, Sun R (2010) Effect of hot-water extraction on alkaline pulping of bagasse. Biotechnol Adv 28:609–612

Li J et al (2012) Homogeneous isolation of nanocellulose from sugarcane bagasse by high pressure homogenization. Carbohydr Polym 90:1609–1613

Mandal A, Chakrabarty D (2011) Isolation of nanocellulose from waste sugarcane bagasse (SCB) and its characterization. Carbohydr Polym 86:1291–1299

Mantanis G, Young R, Rowell R (1995) Swelling of compressed cellulose fiber webs in organic liquids. Cellulose 2:1–22

Premjai P, Khammuang P, Somord K, Tawichai N, Intatha U, Soykeabkaew N (2014) Bio-based composites of sugarcane bagasse: effect of bagasse particle size. In: Paper presented at the 26th annual meeting of the Thai Society for Biotechnology and international conference, Thai Society for Biotechnology (TSB) and Mae Fah Lunag University (School of Science), Chiang Rai, Thailand

Rosa M et al (2010) Cellulose nanowhiskers from coconut husk fibers: effect of preparation conditions on their thermal and morphological behavior. Carbohydr Polym 81:83–92

Saito T, Kimura S, Nishiyama Y, Isogai A (2007) Cellulose nanofibers prepared by TEMPO-mediated oxidation of native cellulose. Biomacromolecules 8:2485–2491

Satari Baboukani B, Vossoughi M, Alemzadeh I (2012) Optimisation of dilute-acid pretreatment conditions for enhancement sugar recovery and enzymatic hydrolysis of wheat straw. Biosyst Eng 111:166–174

Siqueira G, Bras J, Dufresne A (2010) Cellulosic bionanocomposites: a review of preparation, properties and applications. Polymers 2:728–765

Sluiter A, Hames B, Ruiz R, Scarlata C, Sluiter J, Templeton D, Crocker D (2005a) Determination of structural carbohydrates and lignin in biomass. National renewable energy laboratory (NREL). http://www.nrel.gov/biomass/analytical_procedures.html. Accessed 17 July 2015

Sluiter A, Ruiz R, Scarlata C, Sluiter J, Templeton D (2005b) Determination of extractives in biomass. National renewable energy laboratory (NREL). http://www.nrel.gov/biomass/analytical_procedures.html. Accessed 17 July 2005

Sun R (2010) Cereal straw as a resource for sustainable biomaterials and biofuels: chemistry, extractives, lignins, hemicelluloses and cellulose. Elsevier, Oxford

Teixeira EDM, Bondancia TJ, Teodoro KBR, Corrêa AC, Marconcini JM, Mattoso LHC (2011) Sugarcane bagasse whiskers: extraction and characterizations. Ind Crops Prod 33:63–66

Thomas S, Pothan LA (2009) Natural fibre reinforced polymer composites: from macro to nanoscale. Old City Publishing, Philadelphia

Viera RG, de Assunção R, Meireles CDS, Vieira JG, de Oliveira GS (2007) Synthesis and characterization of methylcellulose from sugar cane bagasse cellulose. Carbohydr Polym 67:182–189

Zhang Y, Nypelö T, Salas C, Arboleda J, Hoeger IC, Rojas OJ (2013) Cellulose nanofibrils. J Renew Mater 1:195–211